Релаксация неравновесных квазичастичных возбуждений в сверхпроводнике

Константин Арутюнов

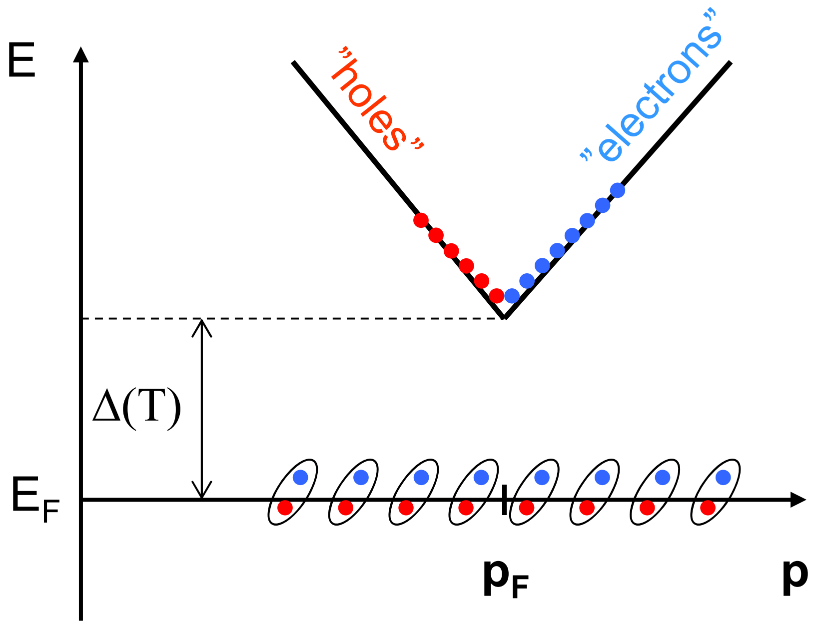

Семинар НУГ 10 ноября 2016

Зонная структура твердых тел

В физике твердого тела одной из главных характеристик является *энергетический спектр*: зависимость энергии электронов проводимости от их импульса E(**p**). В общем случае такие зависимости сложные и форма E(**p**) зависит от направления импульса. Однако, как правило, играют доминирующую роль только те области, где (1) расстояние по энергии между этими разрешенными энергетическими уровнями минимально и (2) граница между заполненными и незаполненными состояниями находится близко с точке схождения.

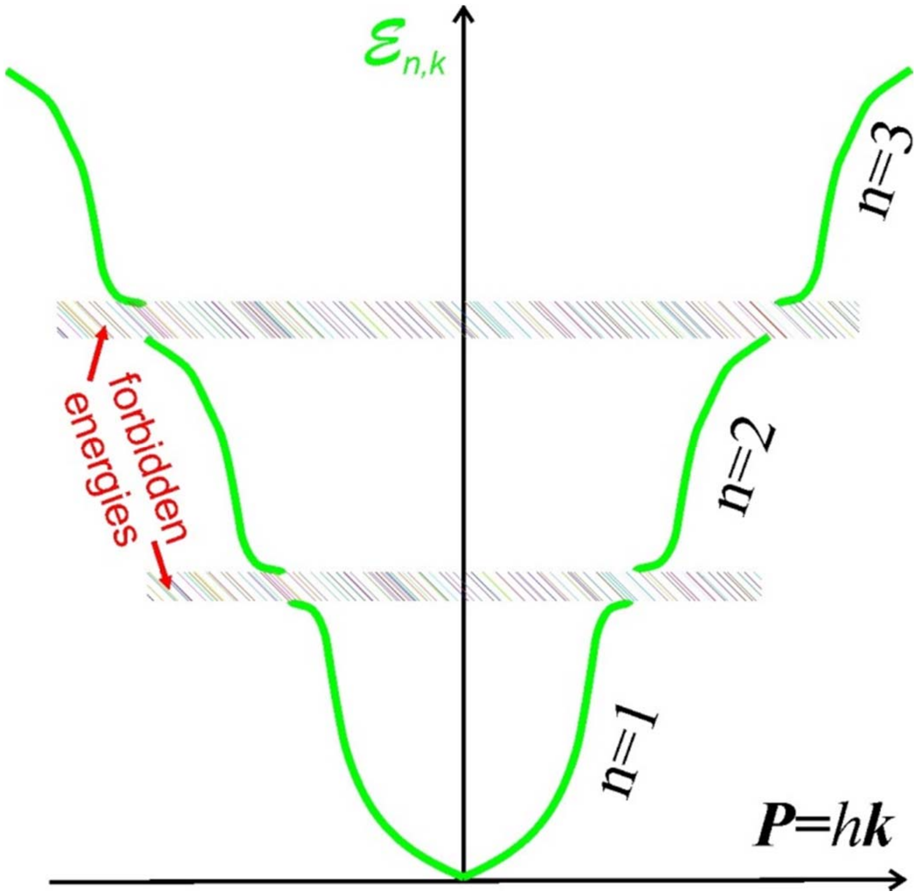

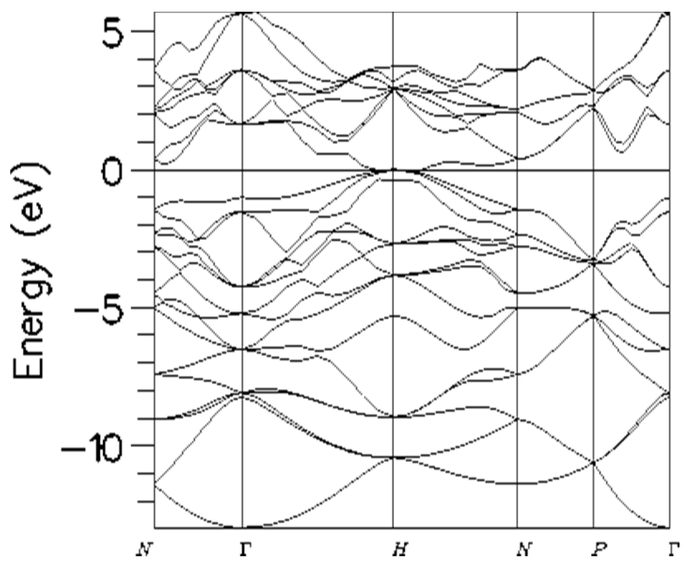

Electronic band structure of silicon in the BC8 structure along several high symmetry lines in the first Brillouin zone of BCC reciprocal lattice. The calculations predict a metallic behavior structure [D. R. Hammann. *Phys. Rev. Lett.*, 42:662, 1979.].

Металлы и диэлектрики

Энергия, разграничивающая свободные от занятых состояний называется *энергией Ферми E_F*, а соответствующий импульс p_F – *Фермиевским импульсом.*

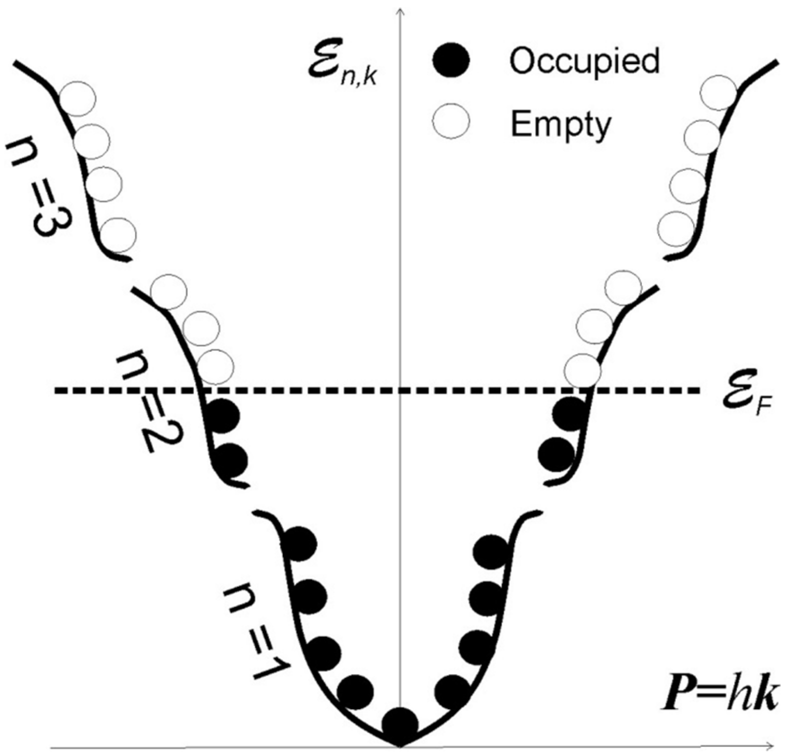

металл

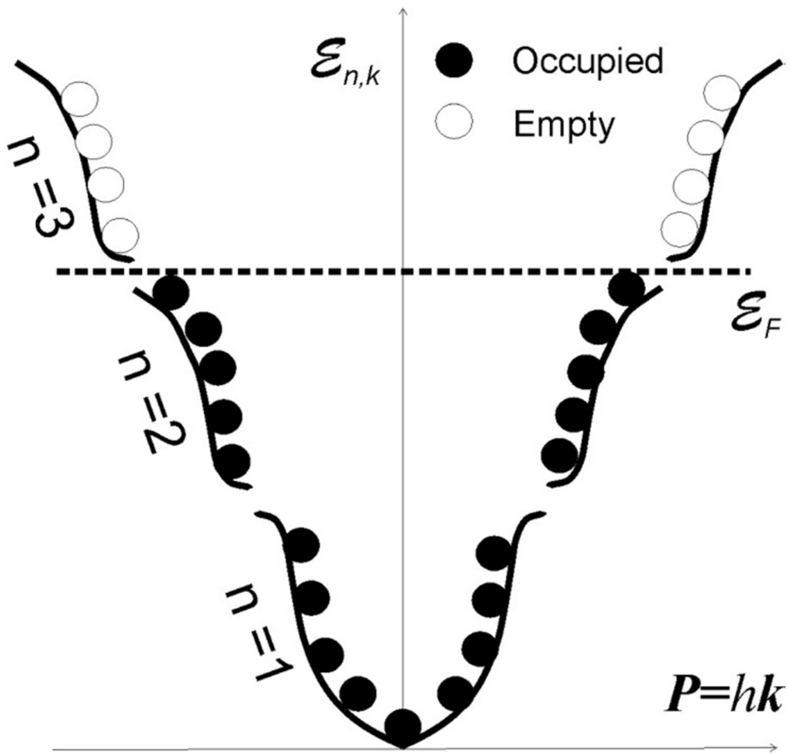

изолятор

Спектр возбуждений

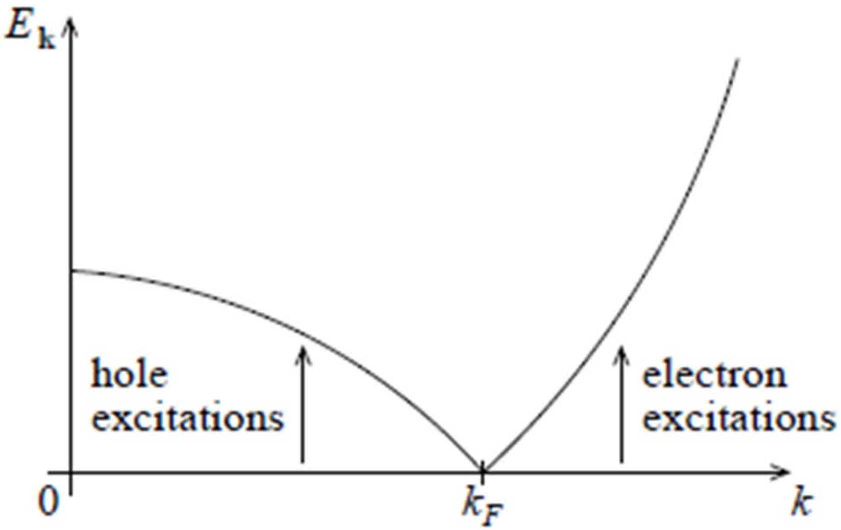

Spectrum of excitations in a normal metal

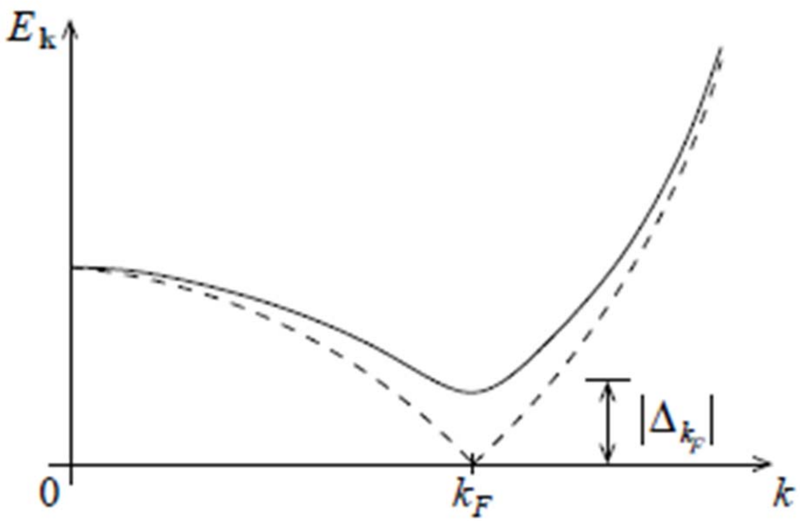

Spectrum of excitations in a superconductor

In a superconductor Cooper pairs occupy the state at Fermi level, while the nearest excited state is separated from the Fermi energy by a supercondcuting gap Δ:

$$|\Delta| = 2\hbar\omega_D e^{-\frac{2}{N(E_F)V}}$$

Плотность состояний сверхпроводника

$$N_s(E) = \begin{cases} N_N(E)\dfrac{2E}{\sqrt{E^2-\Delta^2}}, \text{if } E > \Delta \\ 0, \text{if } E < \Delta \end{cases}$$

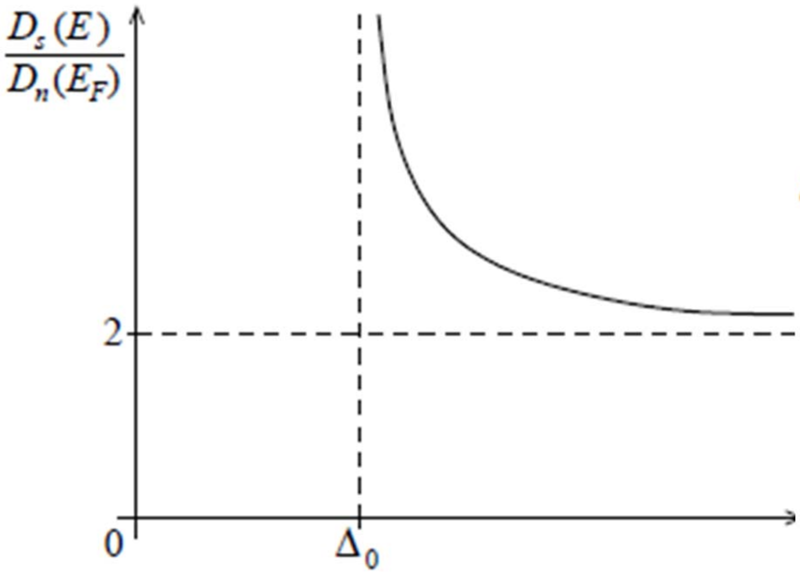

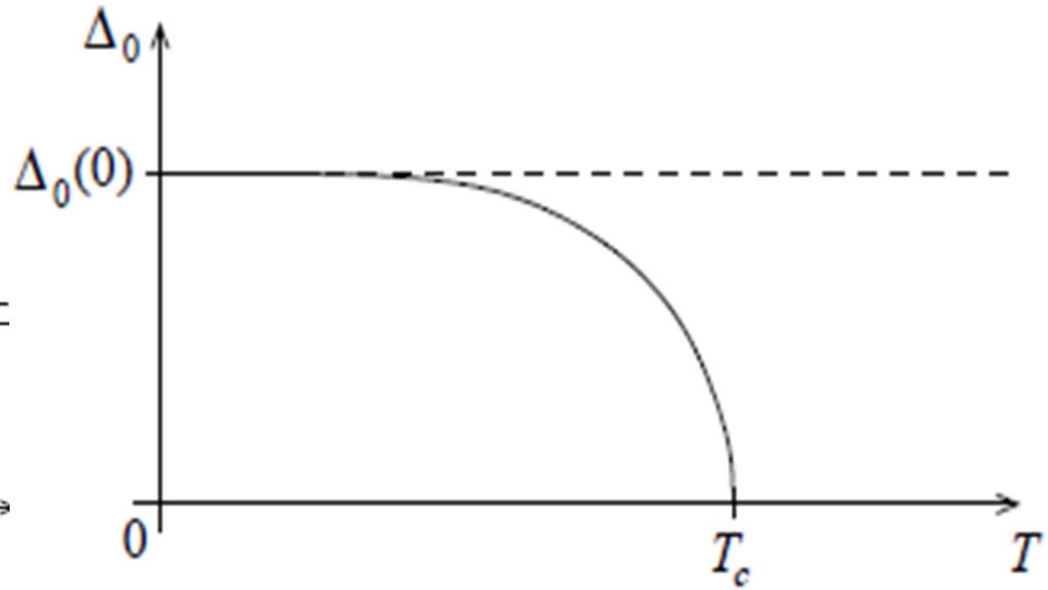

For conventional superconductors
$2\Delta(T=0) = 3.52 k_B T_c$

Outline

- Concept of non-equilibrium quasiparticles

- Relaxation of transverse mode

  charge imbalance → chemical potential shift

- Relaxation of longitudinal mode

  broadening of DOS

  reduction of gap → increase of the effective electron temperature

Quasiparticles

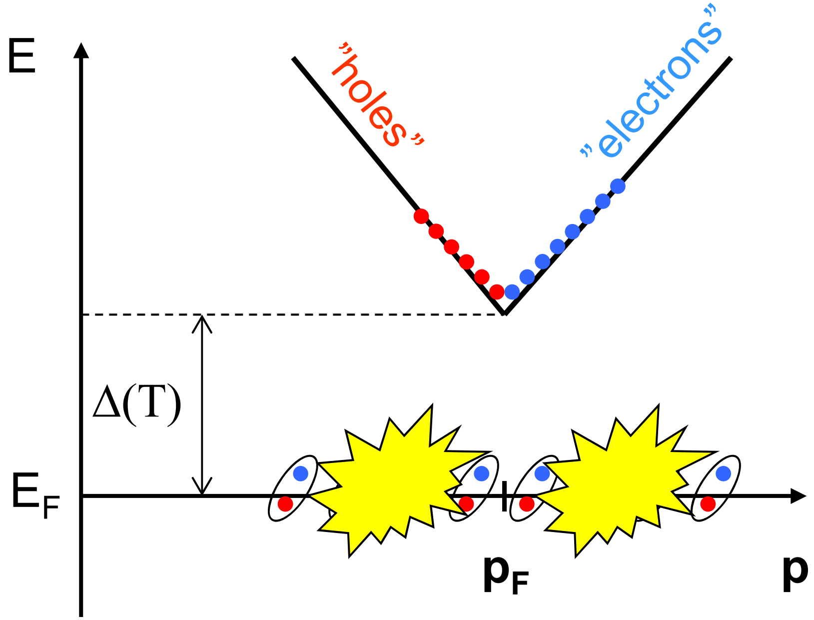

Excitation spectrum of a superconductor

T = 0

T > 0: equilibrium quasiparticles

T > 0: pair breaking

T > 0: quasiparticle injection

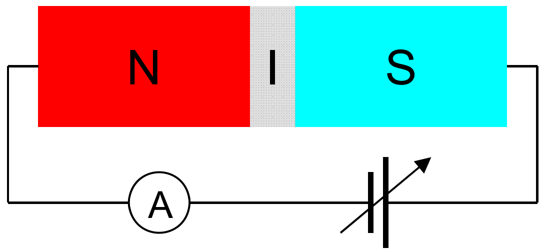

Population of electron-like or hole-like branches depends on the polarity of the injecting voltage:
quasiparticle charge imbalance

Non-equilibrium quasiparticle relaxation

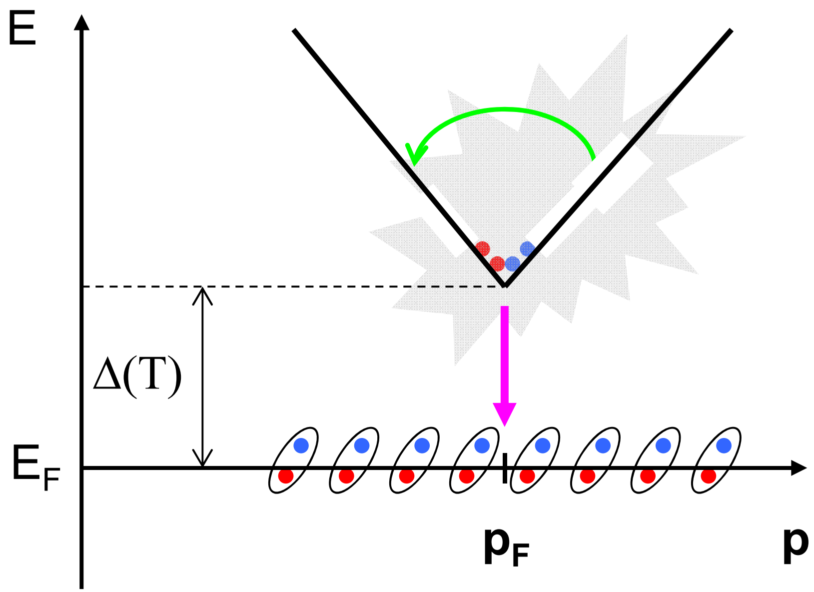

τ_s quasiparticle scattering

τ_Q branch imbalance equalization

τ_R recombination: formation of Cooper pairs

All processes are inelastic[1]: characteristic lifetimes increase at low temperature

[1] If there is anisotropy or spatial variation of the gap elastic processes can contribute to the branch imbalance equalization

What is known about the lifetimes?

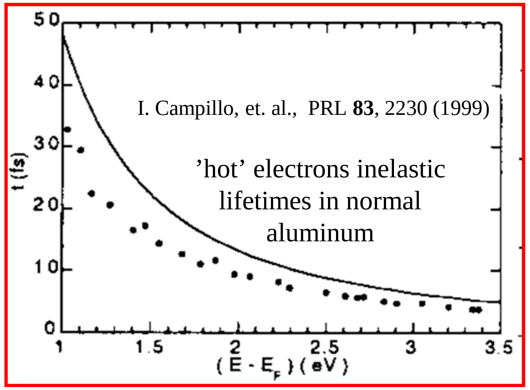

At high excitations E>>Δ scattering of 'hot' electrons is very fast

S. B. Kaplan, et. al., PRB 14, 4854 (1976)

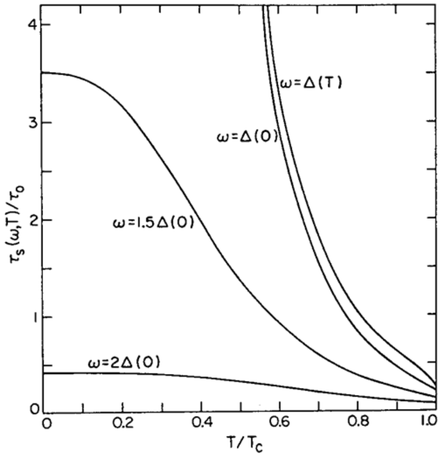

FIG. 1. Scattering lifetime τ_s in units of τ_0 vs T/T_c for quasiparticles with different excitation energies ω. Table I lists τ_0 for various metals. These curves were obtained using the approximation $\alpha^2(\Omega)F(\Omega)=b\Omega^2$.

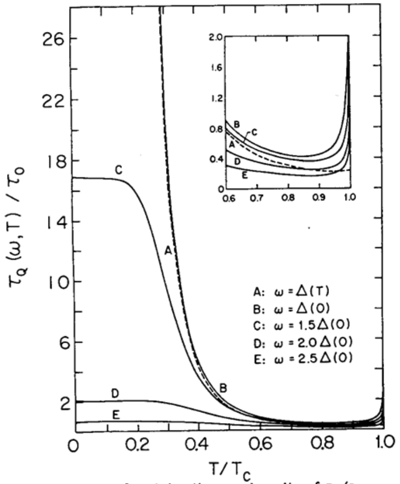

FIG. 11. Branch-mixing time τ_Q in units of τ_0 (see Table I) vs T/T_c for quasiparticles with various excitation energies E. The inset shows an enlargement of the vertical scale for temperatures near T_c. For these curves $\alpha^2(\Omega)F(\Omega)=b\Omega^2$.

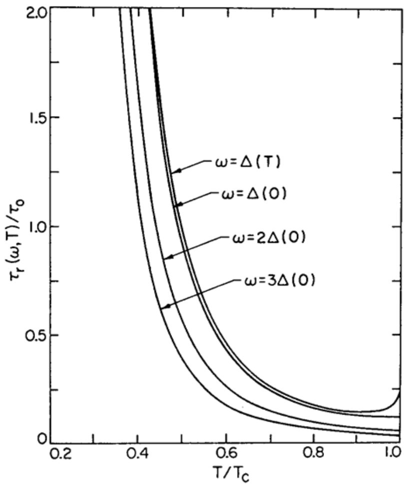

FIG. 2. Recombination lifetime τ_r in units of τ_0 (see Table I) vs T/T_c for quasiparticles with various excitation energies ω. These curves were obtained using the approximation $\alpha^2(\Omega)F(\Omega)=b\Omega^2$.

$\tau_0 \sim 10^{-8}\ s$ is the electron-phonon scattering time for aluminium.

At injection E→Δ and T→T$_c$ the corresponding lifetimes tend to infinity

Existing experiments

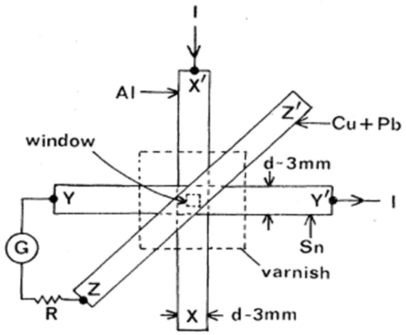

FIG. 1. Sample configuration. In order of deposition, the films are Al (XX'), Sn (YY'), varnish, Cu (ZZ'), and Pb (ZZ'). Galvanometer G and resistor R measure the potential difference V between Y and Z.

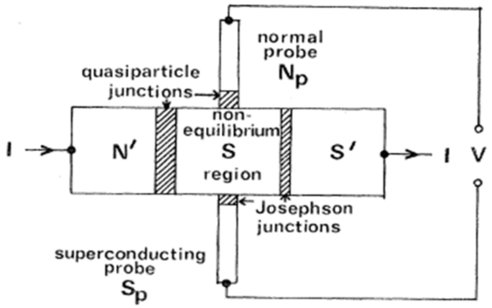

FIG. 1. Schematic diagram of nonequilibrium experiment. Quasiparticles are injected into S from N', and pairs extracted into S'. S_p measures the pair chemical potential in S, while N_p measures the quasiparticle potential.

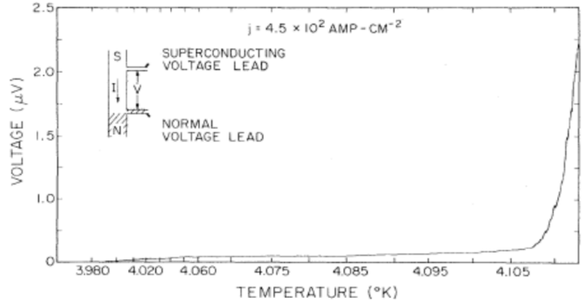

FIG. 1. Potential measured below the superconducting transition of a current-carrying S/N boundary. This potential is zero if the normal probe is superconducting.

J. Clarke, PRL 28, 1363 (1972)
M. Tinkham and J. Clarke, PRL 28,1366 (1972)
M. L. Yu and J. E. Mercerau, PRL 28,1117 (1972)
J. Clarke, B. R. Fjordboge, P. E. Lindelof, PRL 43, 642 (1979)

Mainly:
- T→ T_c limit
- poor spatial resolution

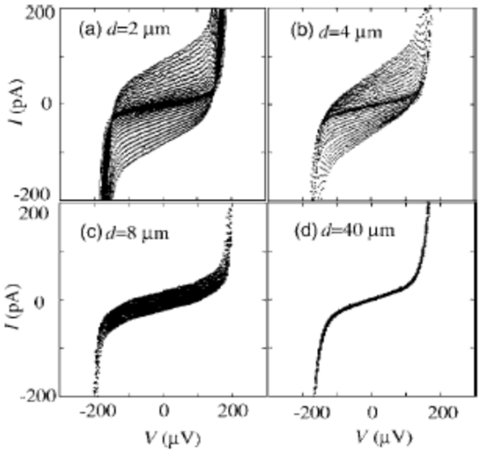

R. Yagi, PRB **73**, 134507 (2006)

Multi-NIS junction structure: observation of variation of the sub-gap current as function of injection current and distance from the remote injector NIS juction

Energy relaxaion of 'hot' quasiparticles in Al:
A.V. Timofeev, et. al., PRL, 102 (2009) 017003; N. B. Kopnin, et. al., arXiv:0905.1210 (2009)

Basic idea of the experiment

Tunnel probes are virtually non-invasive.
Usage of multiple tunnel probes:
G.J. Dolan and L. D. Jackel, PRL 39,1628 (1977)

Our layout:

- ➢better spatial resolution
- ➢ultra-low temperatures
- ➢variation of the injection energy
- ➢symmetric and asymmetric probing

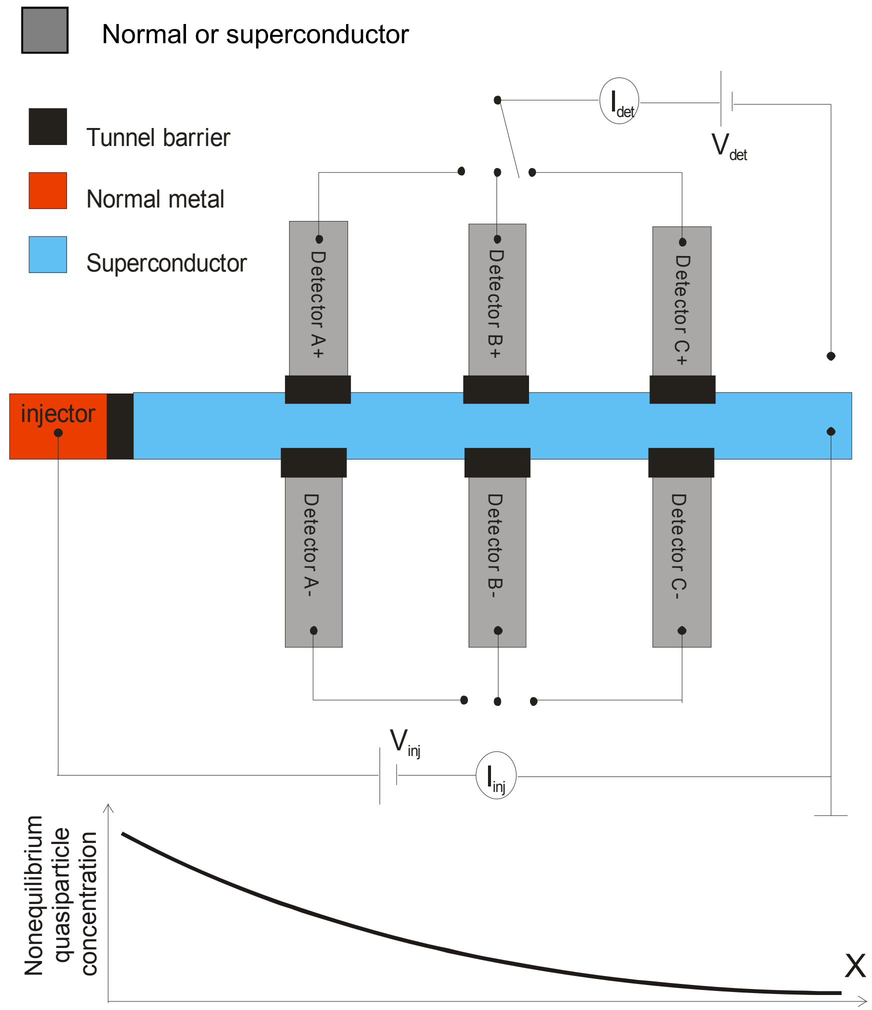

Objective: to determine non-equilibrium DOS and distribution function f_S as functions of temperature T, injector current I_i and the proximity to the injector ΔL_{id}

NIS and SIS probing

NIS_x : detector current depends on the properties of the probed superconductor (S_x) only through its DOS:

$$I_d = \frac{G_{NN}}{e}\int_0^{\infty} \mathrm{N}_x(E,\Gamma)\left[f_N(E) - f_N(E+eV_d)\right]dE$$

S_dIS_x: detector current depends on the properties of the probed superconductor (S_x) both through its DOS and the distribution function $f_x(E)$:

$$I_d = \frac{G_{NN}}{e}\int_0^{\infty} \mathrm{N}_x(E,\Gamma)\mathrm{N}_d(E+eV_d,\Gamma)\left[f_x(E) - f_d(E+eV_d)\right]dE$$

The reduced superconducting DOS $\mathrm{N}(E,\Gamma) = \left|\mathrm{Re}\left(\frac{E+i\frac{\Gamma}{2}}{\sqrt{\left(E+i\frac{\Gamma}{2}\right)^2-\Delta^2}}\right)\right|$, Γ is the pair breaking parameter.

Performing NIS_x and SIS_x experiments of a non-equilibrium superconductor S_x one can disentangle the contributions coming from the DOS and the distribution function

The samples

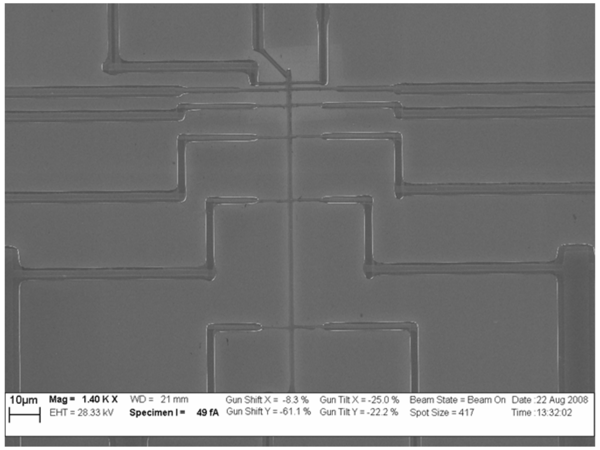

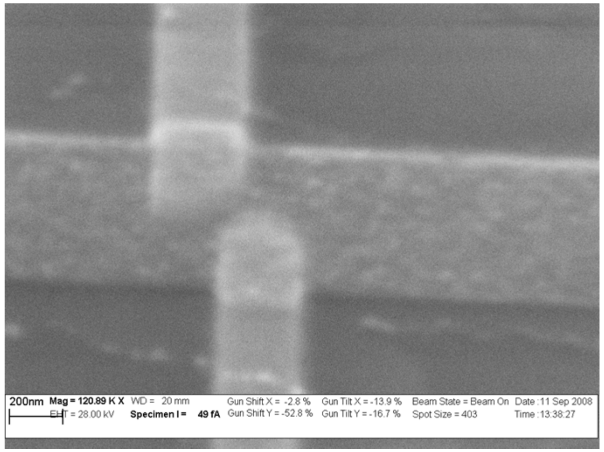

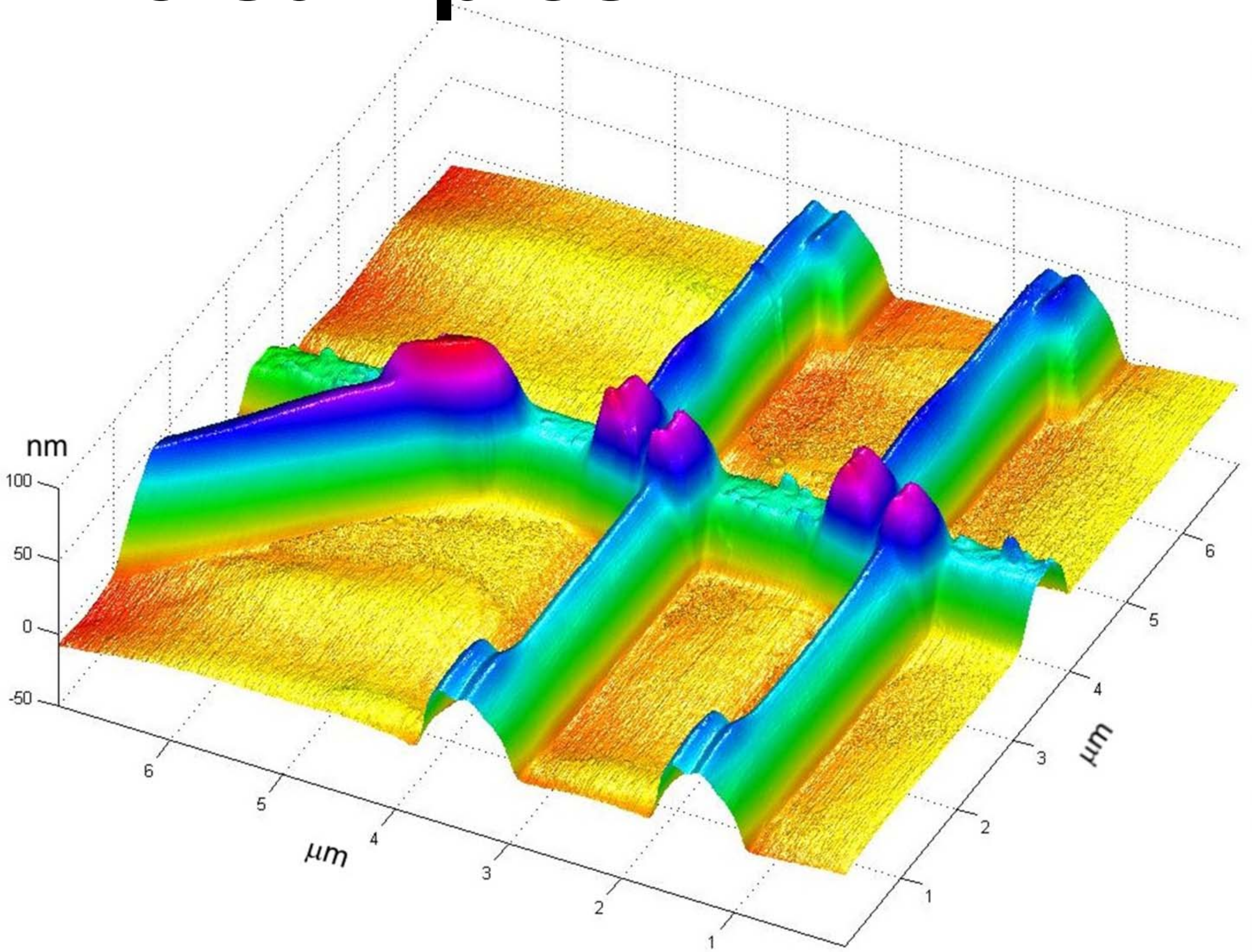

Typical parameters:
Al: d=25 nm, w=400 nm, Cu (detector): d=35 nm, w=300 nm
Cu (injector): d=70 nm, w=1600 nm

Basic assumptions

I. Detector junctions are non-invasive: typically
R^d_T ~ 50 kOhm, R^i_T ~ 5 kOhm

II. Injection current << critical curent: DOS in the superconductor is not broadened due to the pair breaking

III. Injection current does not overheat the normal injector

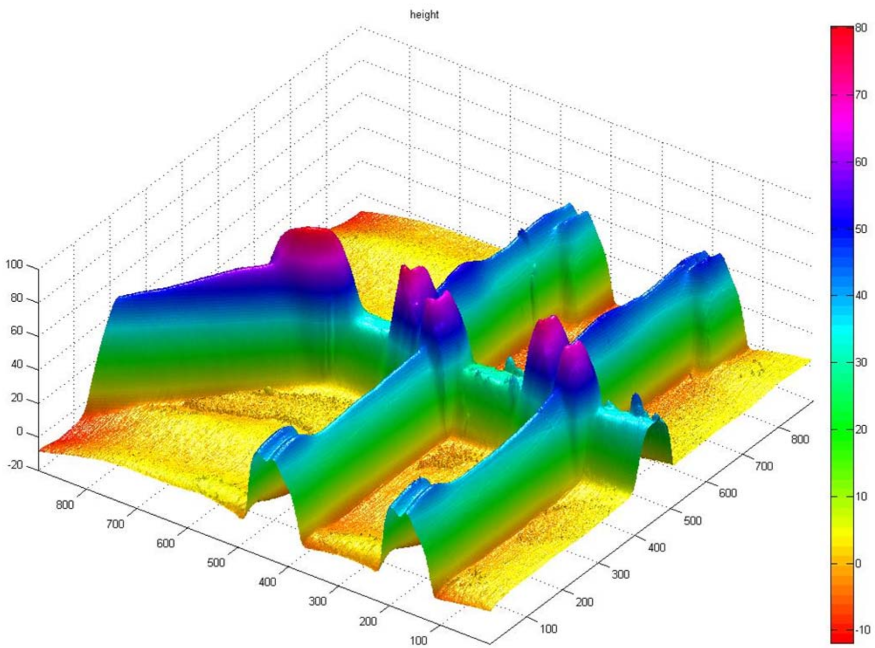

In a separate experiment we measured the electron temperature of the copper injector. In the worst case scenario $T_{bath} \approx 20$ mK and maximum injection energy $eV_{inj} \approx 100\Delta$:

T_e^{max} (injector) ≈ 280 mK

Transverse mode: charge imbalance

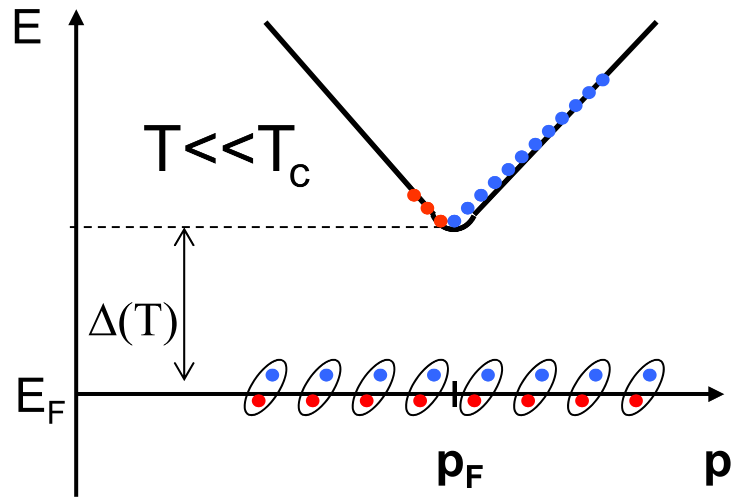

Charge imbalance by tunnel injection

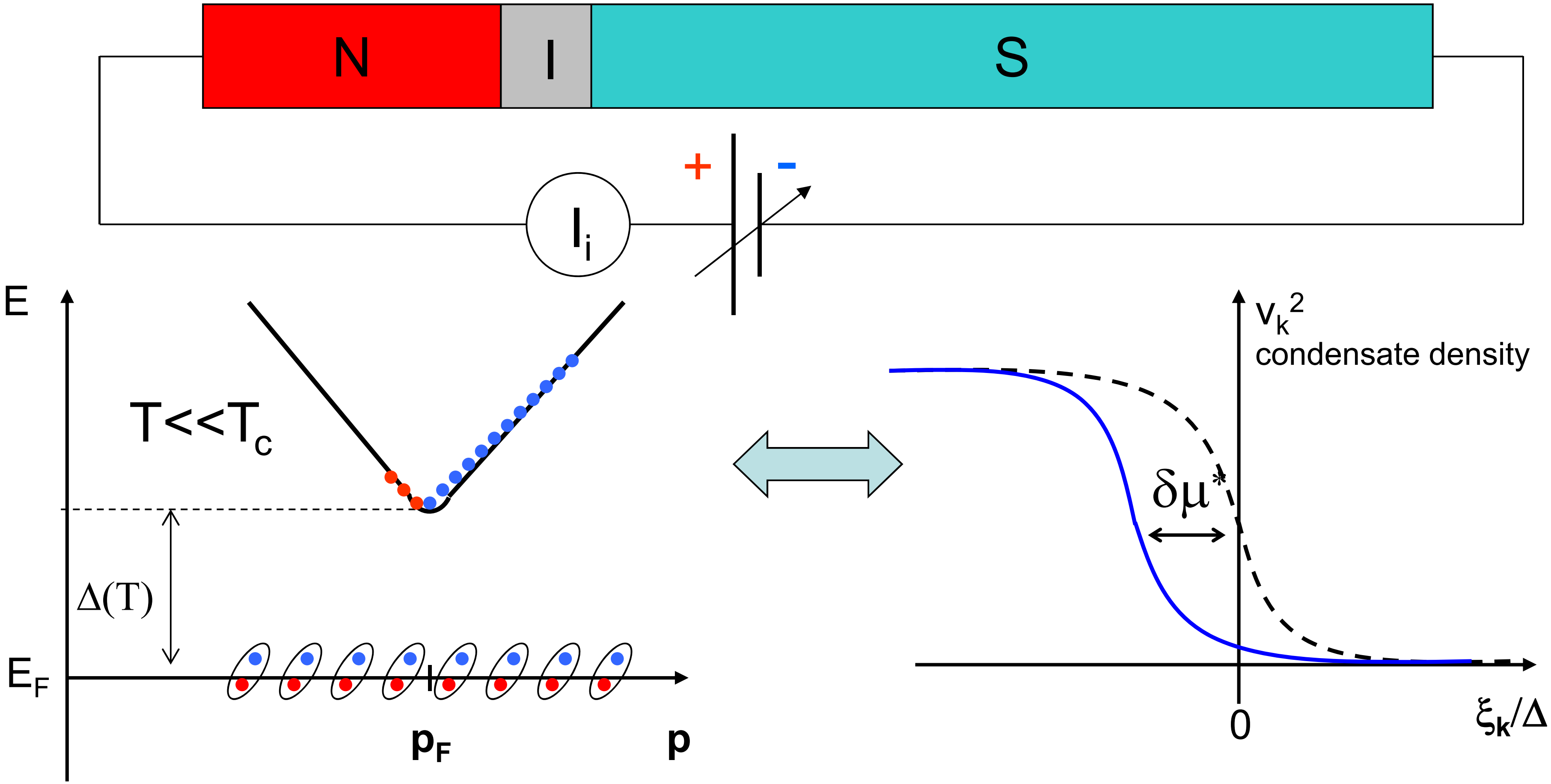

Charge imbalance results in the shift of the pair chemical potential:

ξ_k is refered now to $\mu_s^*=\mu_s - \delta\mu^*$

$$f_S(E) = \frac{1}{\exp\left(\frac{E-\mu^*}{k_B T_e^*}\right)+1}$$

μ* model: C. S.Owen and D. J. Scalapino, PRL 28, 1559 (1972)

Quasiparticle imbalance generated by tunneling

$$I_d = \frac{G_{NN}}{e}\int_0^\infty \left\{ \underbrace{\frac{E}{\left(E^2-\Delta^2\right)^{1/2}}\left[f(E)-f(E+eV_d)\right]}_{\text{equilibrium tunnel current}} + \underbrace{\left(f_{k<}-f_{k>}\right)}_{\text{non-equilibrium}} \right\} dE$$

In equilibrium the tunnel current depends on the properties of the superconducting electrode <u>only</u> through Δ. The thermodynamic temperature explictly enters through the distribution function f.

The non-equilibrium term dependence on energy is complicated. However, at zero voltage bias the equilibrium term cancels contributing to the <u>**excess**</u> current:

$$\delta I_d \equiv I_d(V_d=0) = \frac{G_{NN}}{e}\int_0^\infty \left(f_{k<}-f_{k>}\right) dE$$

Quasiparticle charge :

$$Q^* = 2\int_0^\infty \frac{E}{\left(E^2-\Delta^2\right)^{1/2}}\left(f_{k<}-f_{k>}\right) dE = -2N(0)\mu^* ,$$

where N(0) is the single - spin DOS per unit volume at Fermi energy

M. Tinkham, PRB 6, 1747 (1972)

NIS detection

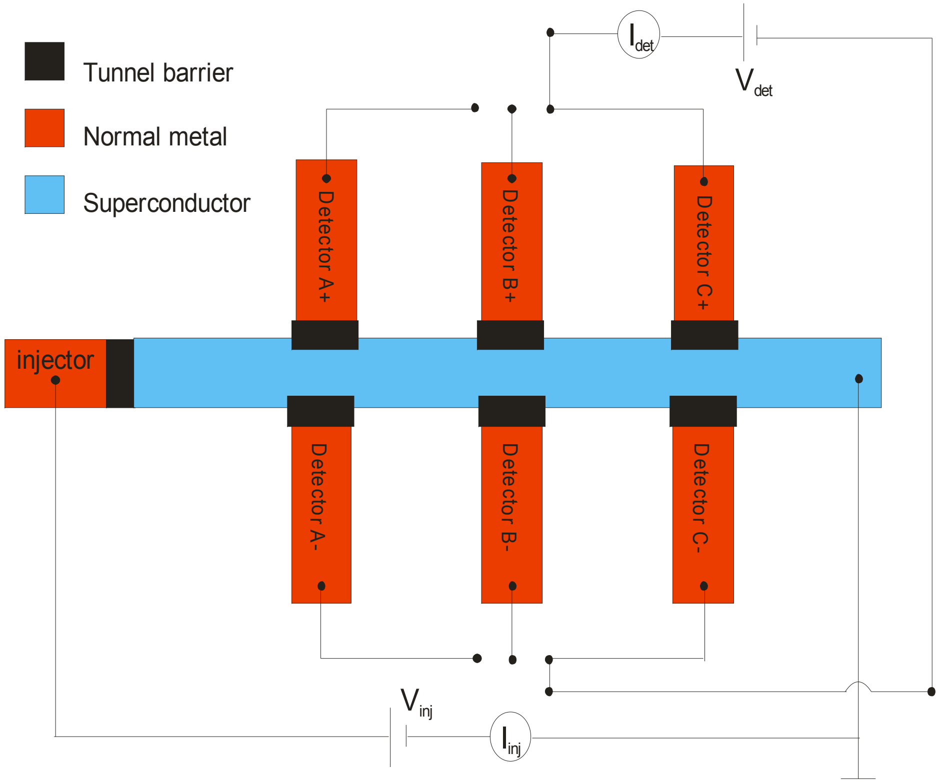

NIS: the detecting signal is measured between one of the detectors and the superconductor

NISIN: the detecting signal is measured between two opposite detectors: to be used for energy relaxation experiments

Expectations for NIS detecting:

- detector's I(V) characteristic should be shifted by δI_d
- δI_d should increase with the injection current I_i
- δI_d should reverse sign with the polarity of I_i
- δI_d should decrease with the distance ΔL_{id}

Excess current

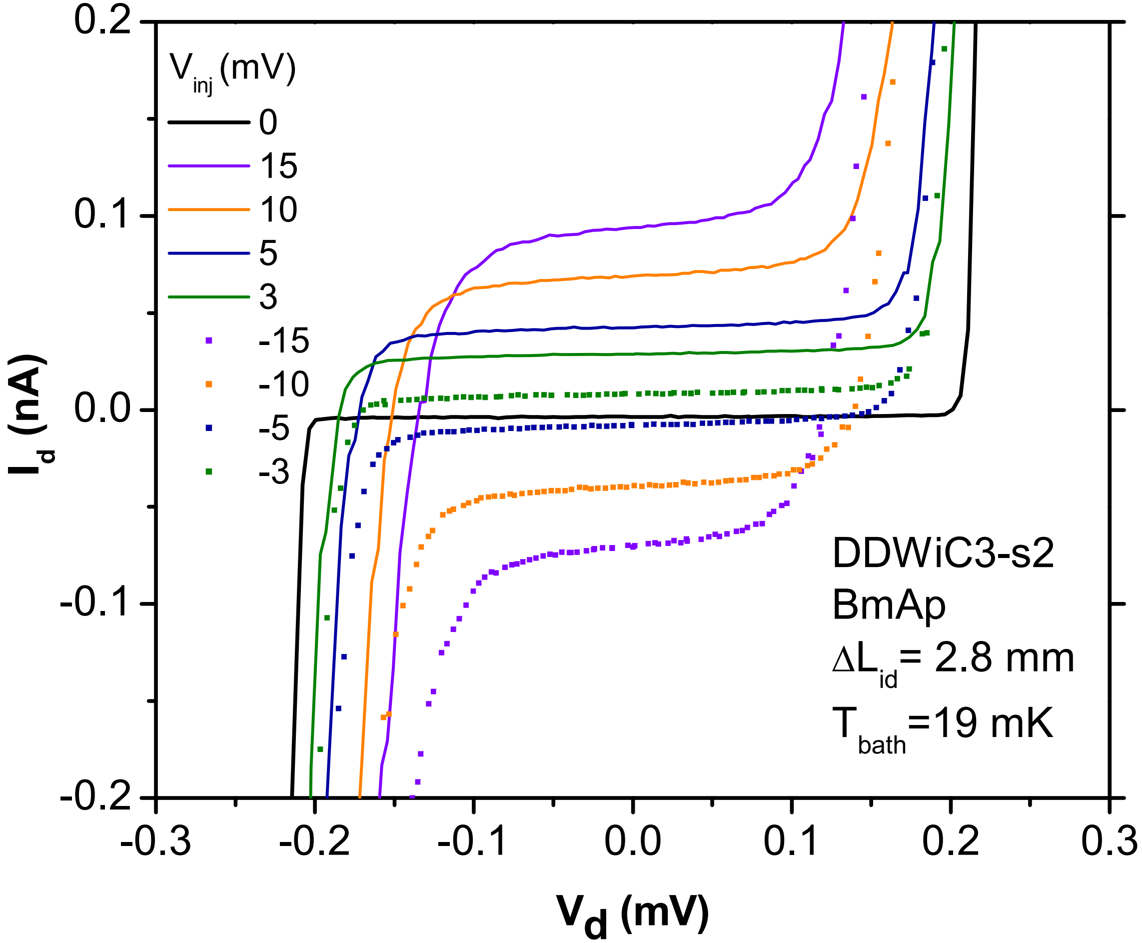

Zoom of a detector's I-V characteristic at sub-gap currents.
With increasing of the injection current the detecor's I(V)s shift in vertical direction: excess current.

Excess current vs. injection energy

The solution of the diffusion equation for the charge imbalance $Q*$ gives the excess current

$$I_d^{ex} = I_i \frac{F^* \Lambda_{Q^*} G^d_{NN}}{2e^2 N(0) D\sigma} \exp(-L_{id}/\Lambda_{Q^*}),$$

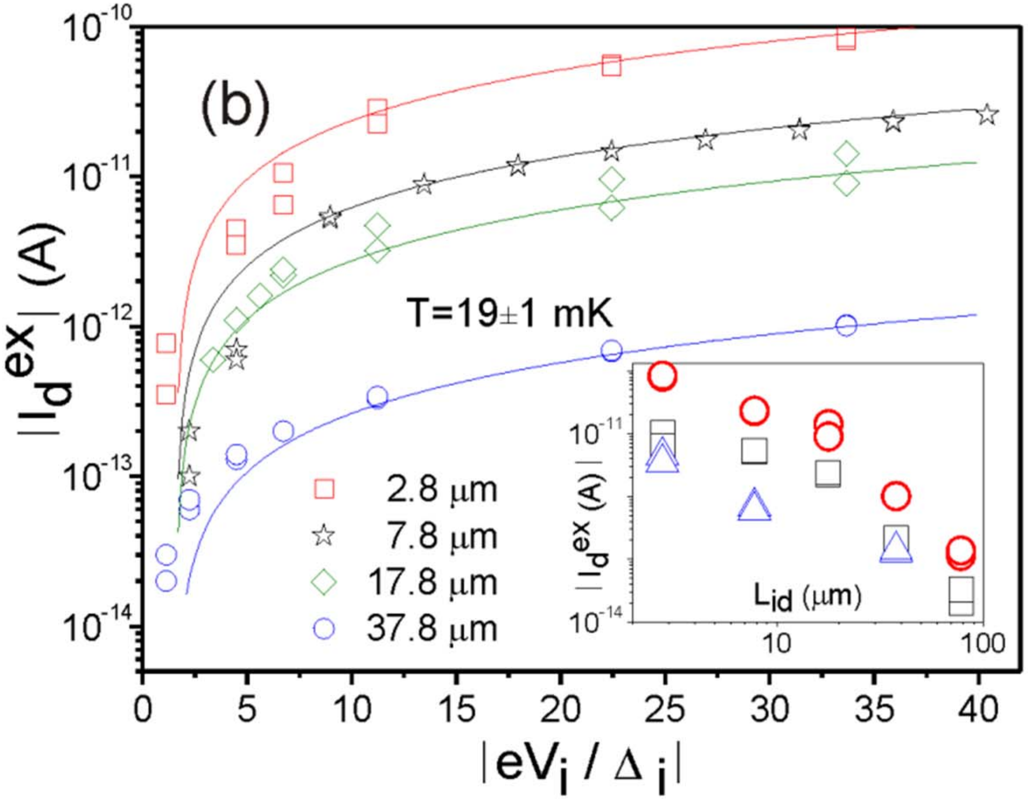

Excess current $I_{ex}{}^{d}$ vs. injection energy eV_i/Δ_i at different distances L_{id} . Lines are fits utilizing λ_{Q*} = 3.6, 3.6, 5.2, and 6.4 μm for the detectors located at L_{id} = 2.8, 7.8, 17.8, and 37.8 μm, respectively. Inset: spatial decay of the excess current measured at | eV_i/Δ_i |= 33.7 (○), 6.7 (□), and 4.5(▲).

Chemical potential shift $\delta\mu^*(V_{inj}, \Delta L_{id})$

$$\delta I_{exc}^{det} = \frac{1}{R_T^{det}} \frac{\delta\mu^*}{e}$$

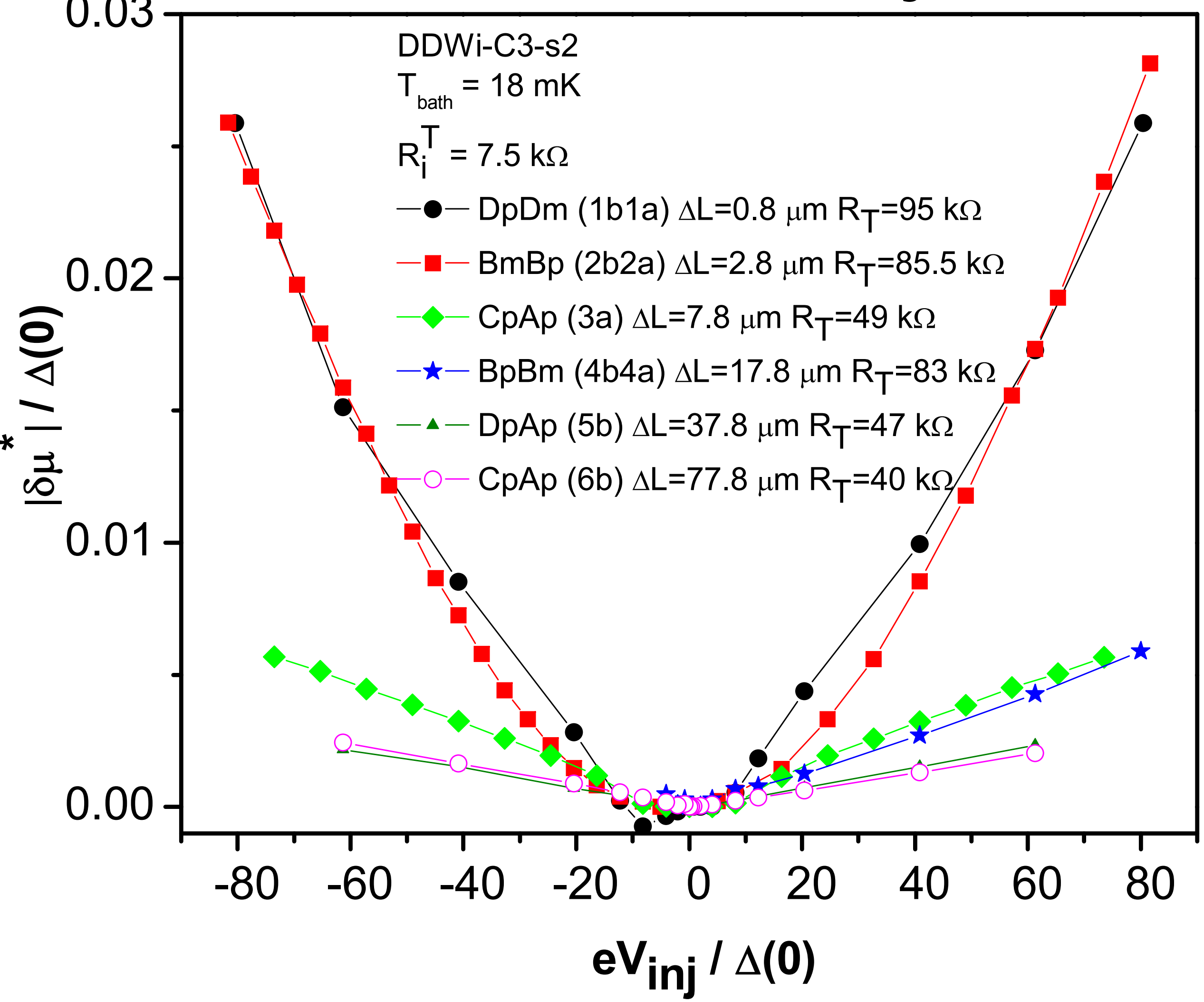

- $\delta\mu^*$ decreases with the distance from the injector
- $\delta\mu^*$ increases with the injector energy
- there is some asymmetry with respect to the injection polarity (thermo-electric effects ?)

Assuming *exp* decay the corresponding relaxation length Λ_{Q^*} = 5±1 μm and the time $\tau_{Q^*} = (\Lambda_{Q^*})^2/D \approx 3$ ns

Chemical potential shift $\delta\mu^*(T)$

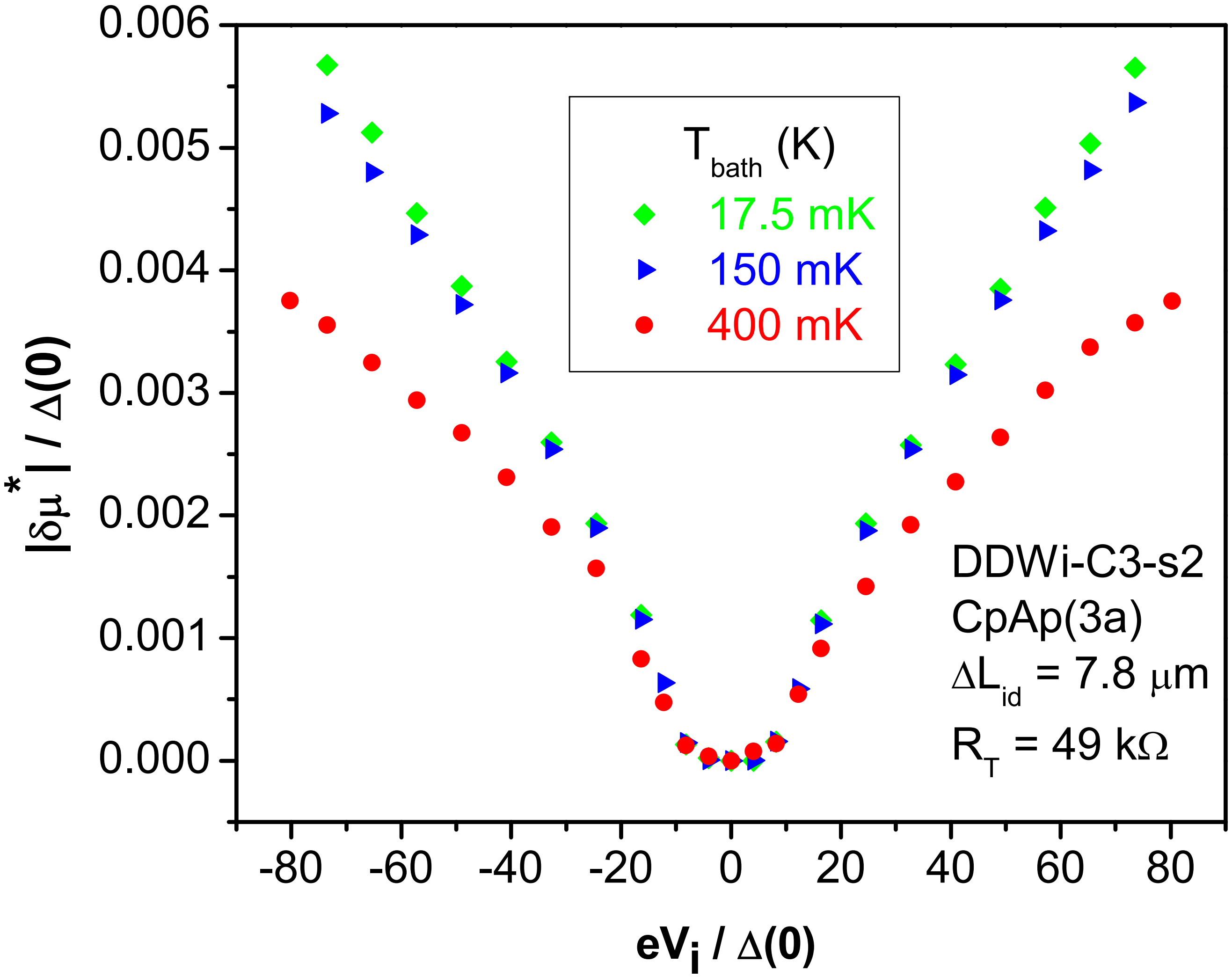

The effect is rather insensitive to temperature at very low temperatures

Longitudinal mode

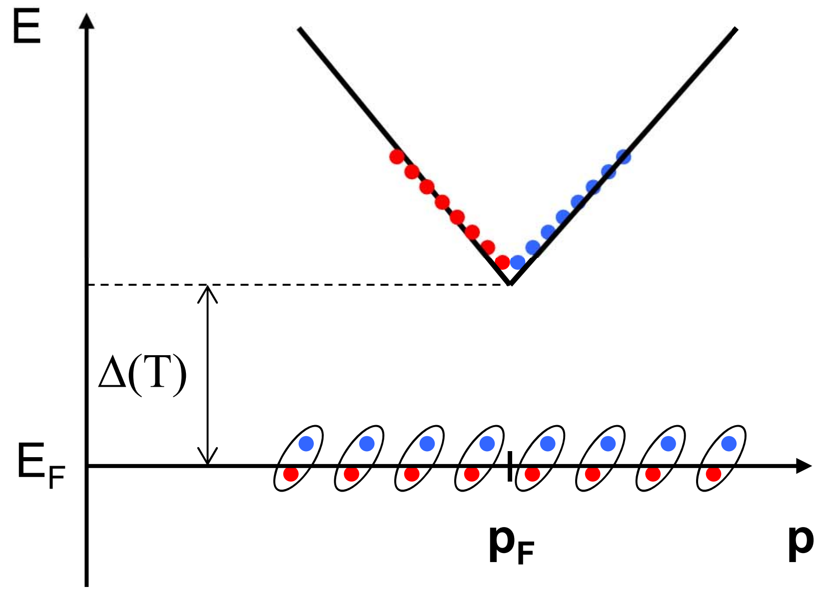

Effective temperature

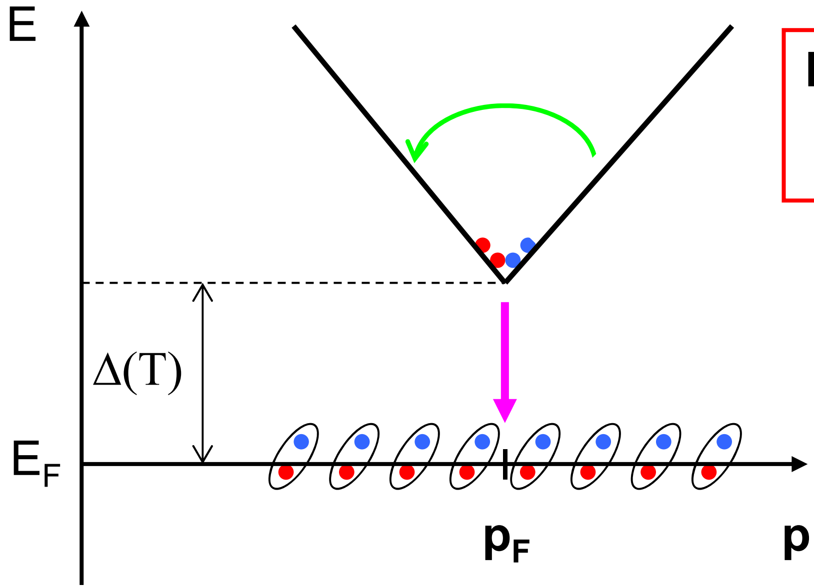

Existence of non-equilibrium quasiparticles

$$T_e^* > T_{bath}$$

$$T_e^* \rightarrow T_{bath}$$

$$f_S(E) = \frac{1}{\exp\left(\frac{E-\mu^*}{k_B T_{e1}^*}\right)+1}$$

Finite charge imbalance

$$f_S(E) = \frac{1}{\exp\left(\frac{E}{k_B T_{e2}^*}\right)+1}$$

After relaxation of the charge imbalance, but before recombination to equilibrium

$$\text{Gap equation}: \frac{1}{\aleph(0)U} = \int_{\Delta}^{\hbar\omega_D} \frac{1-2f_s(E)}{\left(E^2-\Delta(T_{e2}^*)^2\right)^{1/2}} dE$$

W. H. Parker, PRB 12 3667 (1975)

Detector's I-V

Same structure, same injector, but different distances to the detector:

$\Delta L_{id} = 0.8\ \mu m$

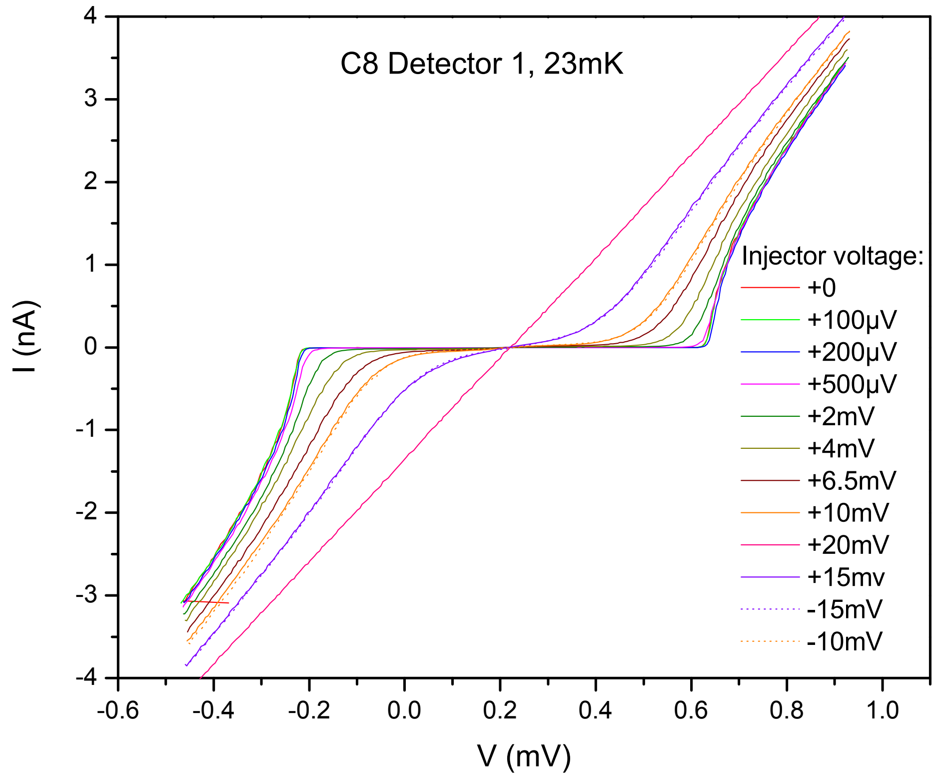

$\Delta L_{id} = 17.8\ \mu m$

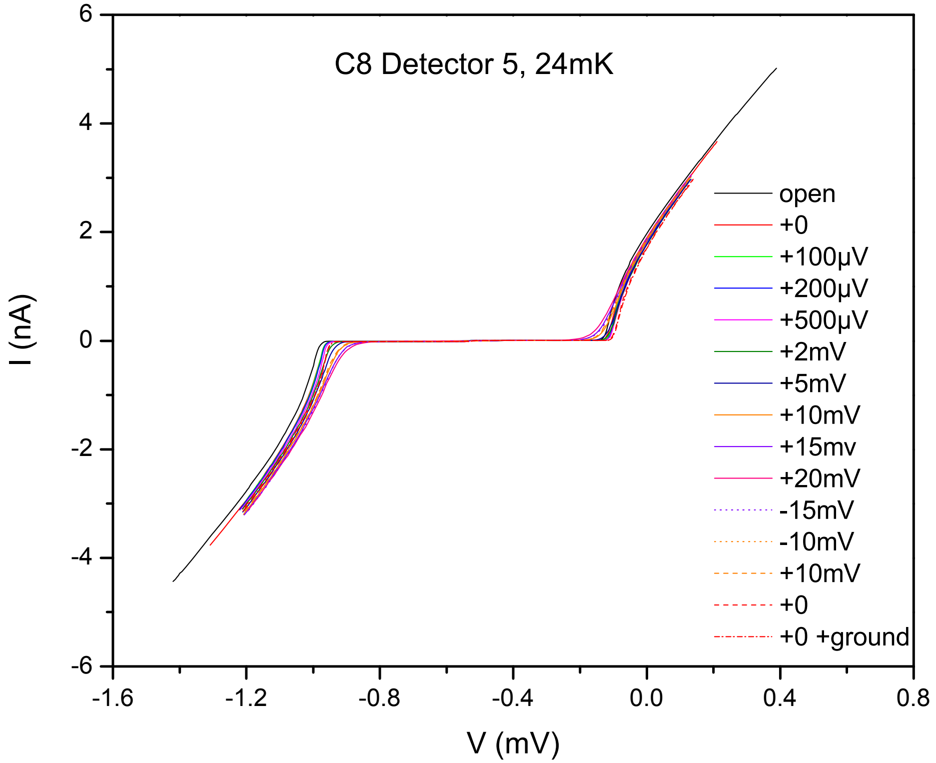

Shape of the detector's I(V) strongly depends on the proximity to the injector and the injection current:

- **superconducting gap is reduced: $\Delta(L_{id}, V_{inj})$**
- **"corners" of the I(V) become rounded: $\Gamma(L_{id}, V_{inj})$**

Dynes DOS broadening Γ

$$N_S(E,\Gamma) = \left| \mathrm{Re}\left\{ \frac{E + i\Gamma/2}{\sqrt{(E + i\Gamma/2)^2 - \Delta^2}} \right\} \right|$$

Finite Γ originates from:

- Magnetic scattering (problematic in Al)
- Proximity effect (not the case: low barrier transparency)
- **Finite quasiparticle scattering time**

[Dynes, et. al., PRL 41,1509 (1978); PRL 53, 2437 (1984)]

In our Al samples at $\Gamma(I_{inj}=0, T<<T_c) / \Delta_0 \sim 1\%$

Fitting experimental data with equilibrium expressions

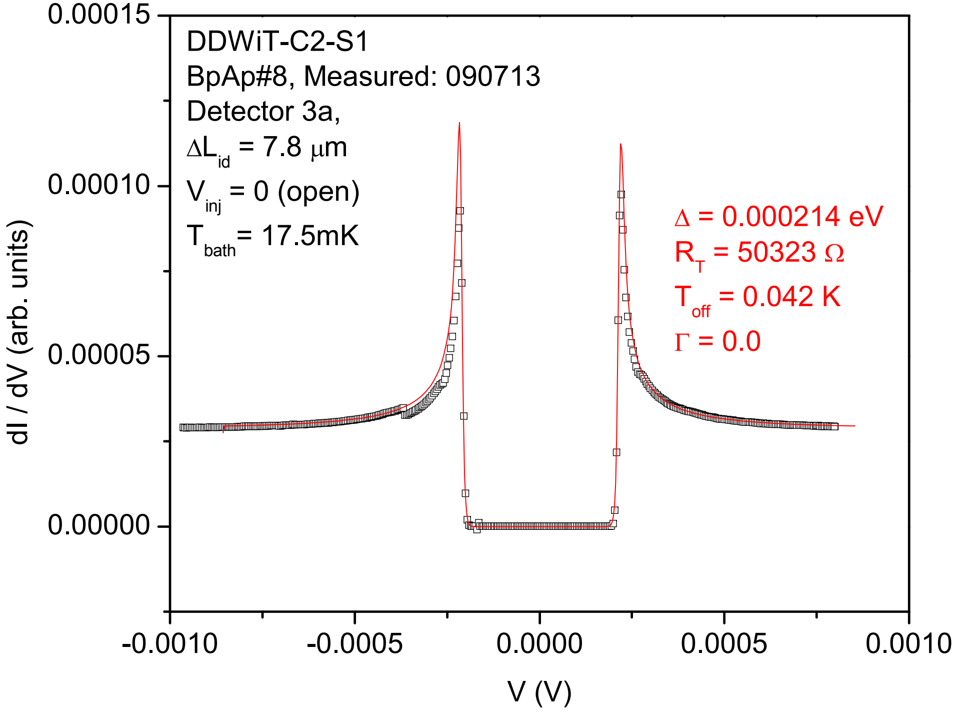

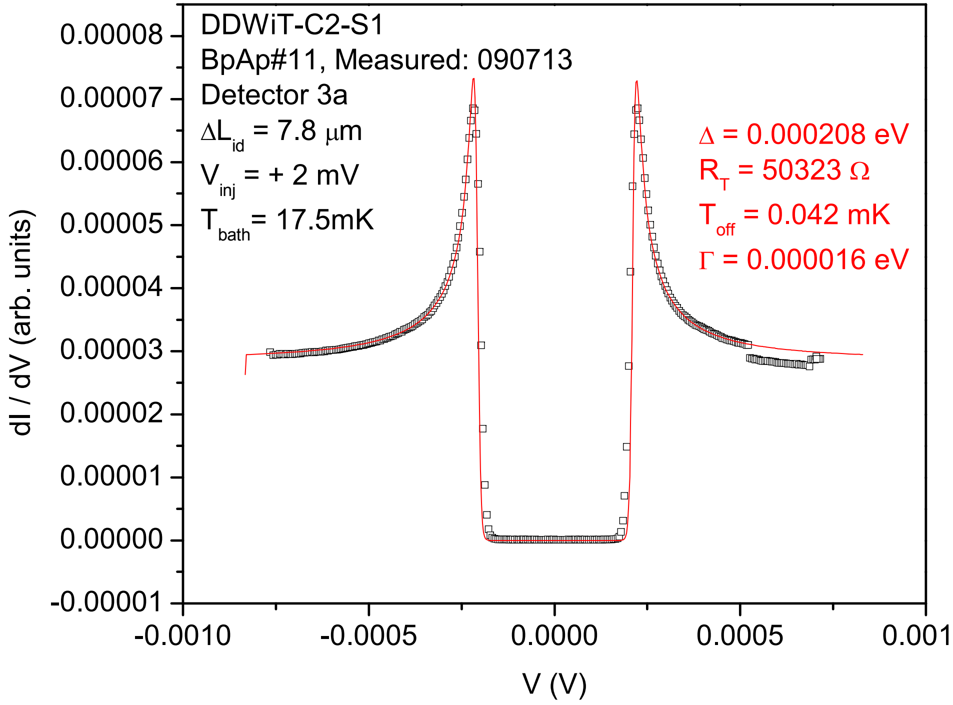

At zero injection the best-fit temperature T_{off} entering the distribution function of the normal detector is always higher than the bath temperature T_{bath} due to inevitable heating coming from the noisy EM environment.

At moderate injection energy ($eV_{inj} \leq 10\Delta$) the shape of experimental dI/dV can be nicely fit by adjusting Δ and Γ keeping the temperature of the normal detector constant $T_N = T_{off} > T_{bath}$.

I(V) fits

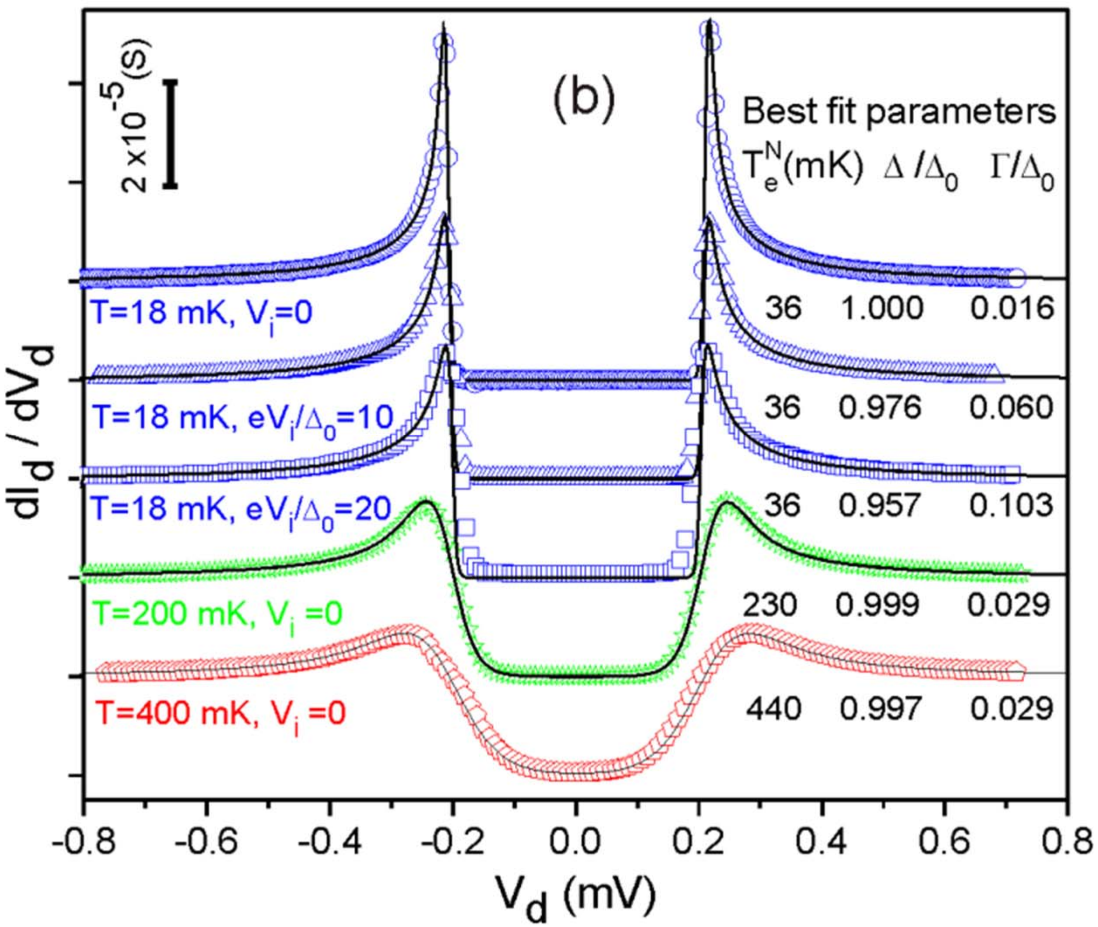

NIS detector located at L_{id} = 2.8 μm experimental dI_d / dV_d dependencies at T = 18 ± 1 mK at various injection energies and at various temperatures. Solid lines are the theoretical best fits with the fitting parameters indicated in the plot.

Note: just the increase of temperature modifies I(V) differently!

DOS broadening $\Gamma(V_{inj})$

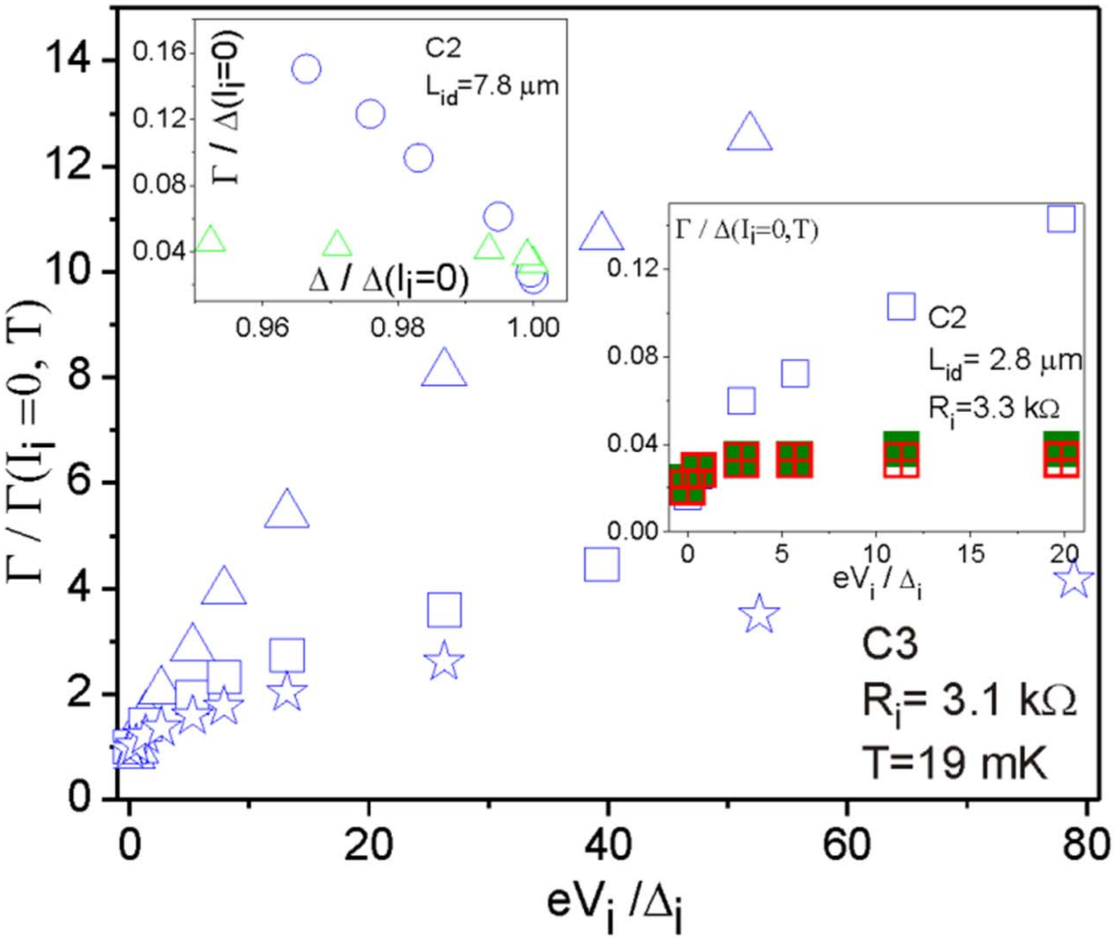

Depairing parameter Γ vs. injection energy for three detectors at L_{id} = 0.8 (▲), 2.8 (□), and 7.8 (star) μm. Left inset: detector located at L_{id} = 7.8 μm $\Gamma(I_i)$ vs.$\Delta(I_i)$ at various injection currents I_i at T = 18 mK (○) and T = 200 mK (▲). Right inset: Γ vs. injection energy at L_{id} = 2.8 μm at T = 17.5 (□), 200 (■), and 400 mK (crossed square).

Suppression of the gap Δ

If a superconductor distrinution function is symmetric (e.g. Fermi) the tunnel current does not depend on the superconductor temperature T_s*.

However, the increase of the effective temperature $T_s^* > T_{bath}$ due to quasiparticle injection can be accounted through suppression of the gap which enters the DOS: $\Delta(T_s^*) < \Delta(T_{bath})$ with.

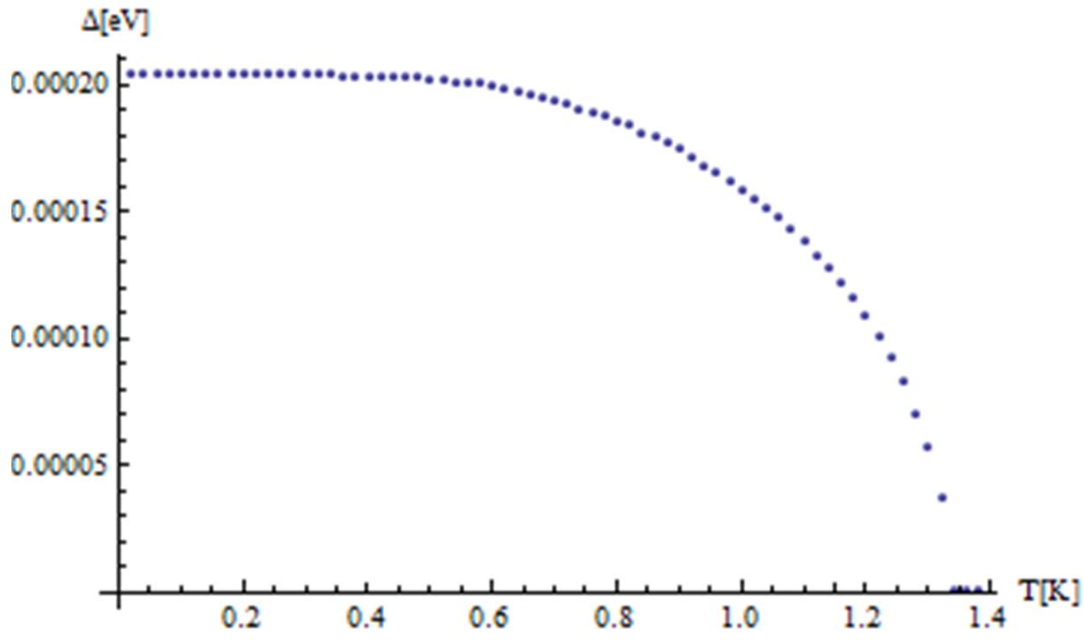

Calculated Δ(T) for aluminium

T_s* is just a convenient parameter of dimensionality ’energy’ and has no direct relation to thermodynamic temperature of a nonequlibrium superconductor

$\Delta(I_{inj}, T)$

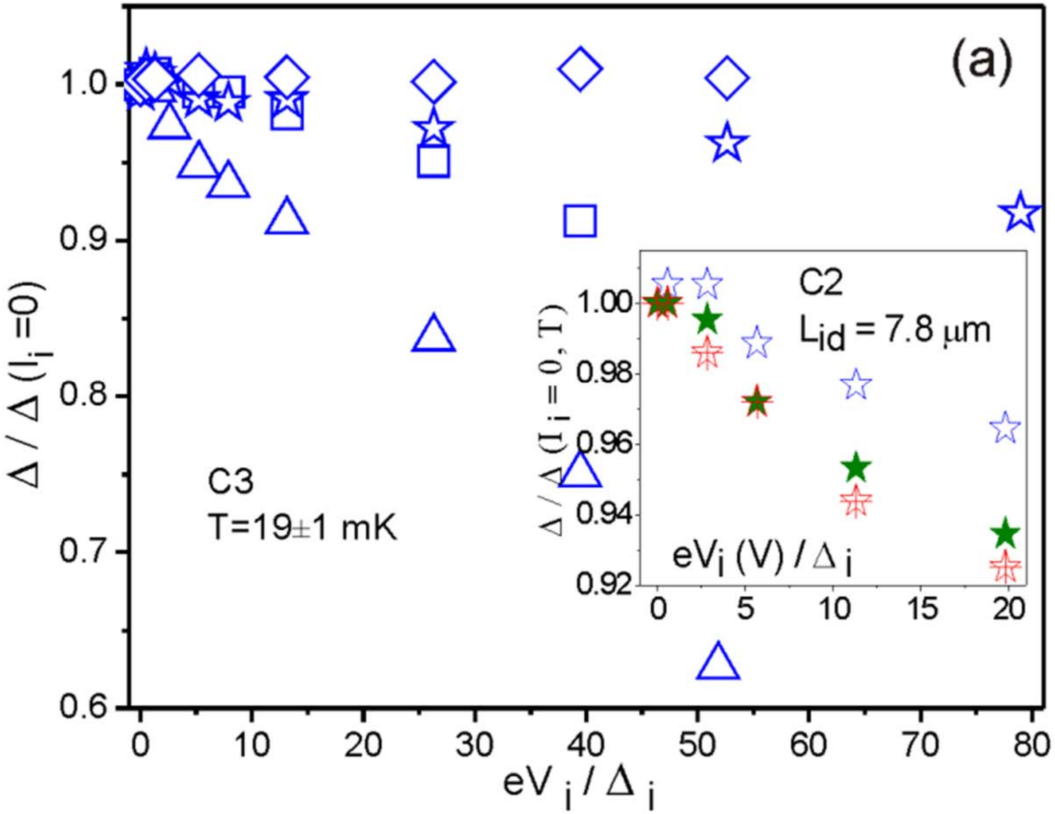

Superconducting gap Δ vs. injection energy at L_{id} = 0.8 (▲), 2.8 (□), 7.8 (star), and 17.8 (◊) µm. Inset: reduction of the superconducting gap measured by the same NIS detector at L_{id} = 7.8 µm at T = 17.5 (open star), 200 (filled star), and 400 (crossed star) mK.

Clear decrease of Δ with increase of the injection energy
The effect is rather insensitive to temperature

ΔT_e^* (injection current)

$\delta T^* \neq I_{inj}^2$
not a trivial Joule heating!
The effect is more pronounced for detectors closer to the injector

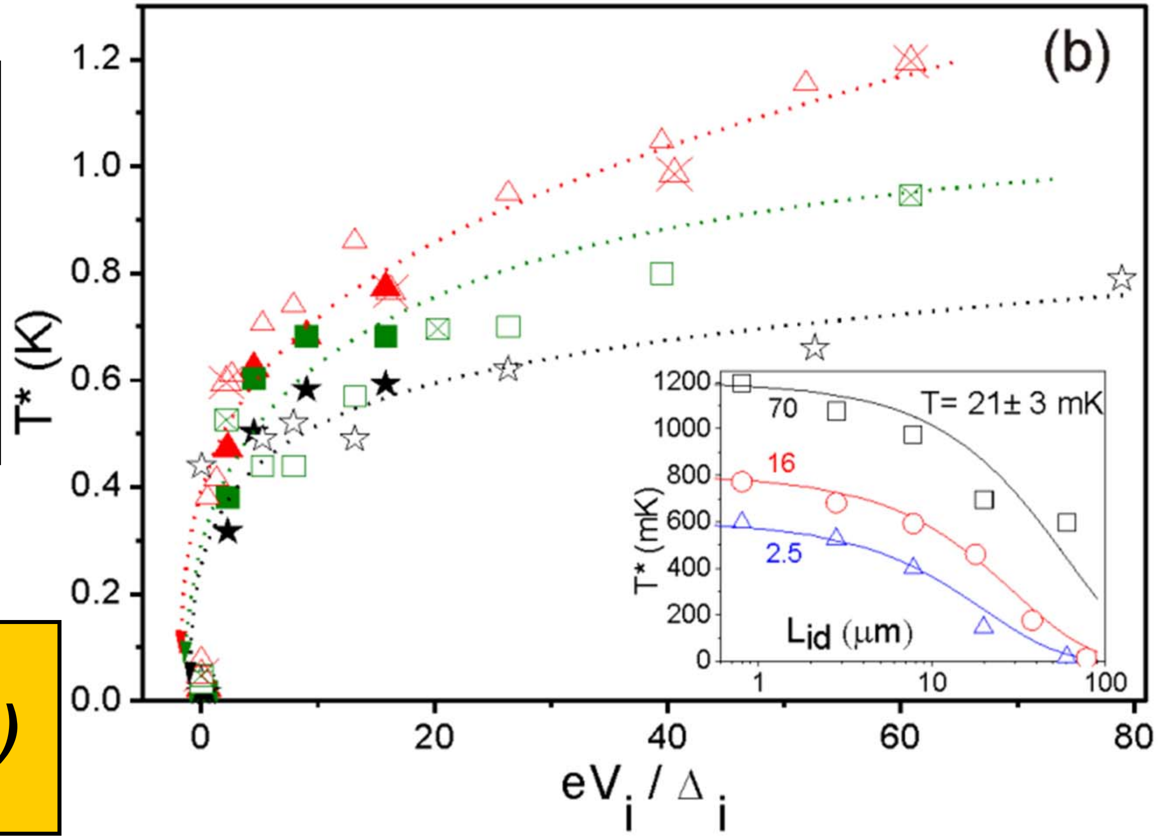

Best fit $\Lambda_T^* \sim$ *40 μm (!)*

Effective temperature T^* vs. injection energy for samples C3 (18 mK, open symbols), C2 (19 mK, solid symbols), and C8 (24 mK, crossed symbols) at L_{id} = 0.8 (▲), 2.8 (□), and 7.8 (star) μm. Lines are guides to the eye. Inset: spatial decay of T^* averaged over several samples at eV_i/Δ_i = 70 (□), 16 (○), and 2.5 (▲). Lines are fits assuming exponential dependence $\sim \exp(-L_{id}/\Lambda_{T^*})$.

Breakdown of equilibrium fittings $\Delta(T^*)$ and $\Gamma(T^*)$

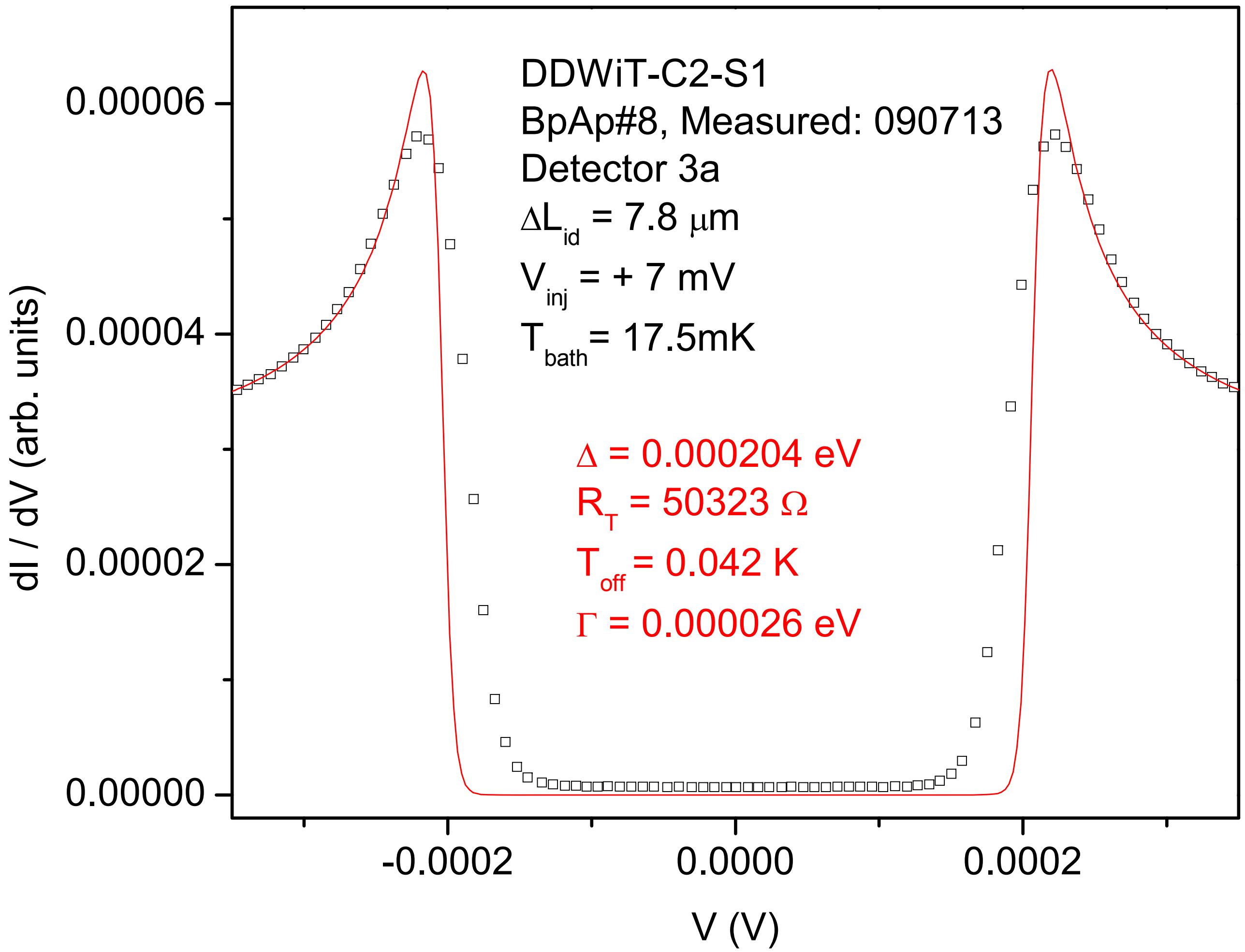

To fit the experimental data at high injection energies ($eV_{inj}>10\Delta$) it is not sufficient to vary only Δ and Γ keeping the temperature of the normal electrode at the offset temperature slightly higher than T_{bath}. Presumably at this high injection limit only the essentially non-equilibrium expressions for the tunnel current should be utilized.

Conclusions

Clear dependence of the detector's I(V) on the injection current, proximity to the injector and temperature

The effects can be qualitatively understood by creation of the chemical potential shift, the increase of the electron effective temperature and DOS broadening

The corresponding relaxation lengths are:
~ 5 μm for the charge imbalance (transverse mode)
~ 40 μm for the effective temperature (longitudinal mode)

Theoretical support is necessary to account for the non-equilibrium distribution function!

Thank you!

Phys. Rev. B 83, 104509 (2011)